

Publication IV

Manuscript reprinted from Progress in Photovoltaics 14(2006), p. 329-340

Data filtering methods for determining of performance parameters in photovoltaic module field tests

Thomas Carlsson, Kim Åström, Petri Konttinen, Peter Lund

Abstract

Evaluating the performance of photovoltaic modules with high precision during field testing is difficult since performance parameters are influenced by several factors, including some which are normally not measured. This work shows that data filtering based on four basic measurement parameters can improve the precision markedly by restricting the analysis to well-defined measurement conditions. Field measurement data from CIGS photovoltaic modules was filtered and analyzed, and a methodology for selecting the best filtering criteria was developed. A comparison to a traditional method shows that the variance in the data can be reduced by as much as 70-80% with suitable filtering conditions. The same filtering reduces the amount of data points by 50%. The method also includes a calculation of temperature coefficients which takes into account time-dependent changes in performance parameters. The results presented in this paper can be used as a tool for planning field tests of photovoltaic modules, for versatile analyses of measured data and for the detection of changes in performance parameters at an early stage of field testing.

Keywords: photovoltaics, field test, data filtering, temperature coefficients, CIGS

Nomenclature

| | |
|------------|--|
| A_Y | zero order time dependence coefficient for Y_{REF} |
| B_Y | first order time dependence coefficient for Y_{REF} |
| C_Y | second order time dependence coefficient for Y_{REF} |
| d | general symbol for any day |
| f | proportion of days with data available, a function of Ω [-] |
| f_A | proportion of days with data available, method A [-] |
| f_B | proportion of days with data available, method B [-] |
| FF | fill factor [-] |
| G | plane-of-array irradiance [W/m^2] |
| G_D | diffuse horizontal irradiance [W/m^2] |
| G_H | global horizontal irradiance [W/m^2] |
| G_{max} | maximum plane-of-array irradiance [W/m^2] |
| G_0 | plane-of-array irradiance filtering parameter [W/m^2] |
| ΔG | plane-of-array irradiance interval filtering parameter [W/m^2] |
| I_{mpp} | maximum power point current [A] |
| I_{sc} | short-circuit current [A] |
| m | general symbol for any module |
| P_{mpp} | maximum module power [W] |
| R | G_H/G_D ratio [-] |
| R_{min} | G_H/G_D ratio filtering parameter [-] |
| r^2 | coefficient of determination [-] |
| SS | sum of squares |
| T | module temperature [$^{\circ}C$] |
| T_{max} | module temperature filtering parameter [$^{\circ}C$] |
| T_{min} | module temperature filtering parameter [$^{\circ}C$] |

| | |
|----------------------------------|--|
| t | time [months] |
| T_{REF} | reference temperature [$^{\circ}C$] |
| V_{mpp} | maximum power point voltage [V] |
| V_{oc} | open-circuit voltage [V] |
| V_Y | residual variance in Y [-] |
| V_Y^A | residual variance in Y obtained with method A [-] |
| V_Y^B | residual variance in Y obtained with method B [-] |
| Var | variance [-] |
| Y | general symbol for I_{mpp} , V_{mpp} , I_{sc} , V_{oc} , I_{mpp}/G or I_{sc}/G |
| Y_{REF} | value of Y at reference conditions |
| α_Y | temperature coefficient of Y [$\%/^{\circ}C$] |
| $\sigma_Y(\Omega, m, d)$ | module- and day-specific standard deviation in Y with filter Ω [%] |
| $\overline{\sigma_Y}(\Omega, m)$ | average of $\sigma_Y(\Omega, m, d)$ over all days [%] |
| $\overline{\sigma_Y}(\Omega)$ | average of $\overline{\sigma_Y}(\Omega, m)$ over all modules [%] |
| θ | sunlight angle of incidence [$^{\circ}$] |
| θ_{max} | sunlight angle of incidence filtering parameter [$^{\circ}$] |
| θ_{min} | sunlight angle of incidence filtering parameter [$^{\circ}$] |
| Ω | a specified combination of filtering criteria |

1. Introduction

Knowledge of the useful lifetime of photovoltaic (PV) modules facilitates the prediction of electricity price for a given PV system and makes it possible to issue suitable warranties to products. Field testing of PV modules is one of the most important methods for confirming that their performance remains stable up to a required lifetime of 20-30 years. If degradation mechanisms are identified in field tests, module manufacturers can improve and test module stability by using relevant accelerated ageing tests in the laboratory [1]. A convenient duration for a field test sequence is 5 years at the most, in which time the performance stability of the tested modules should be verified and possible problems identified. A short feedback cycle between field testing and laboratory testing is of particularly high value for new and rapidly evolving PV technologies such as thin-film Cu(In,Ga)Se₂ (CIGS), since the performance stability of thin-film modules can depend to a significant degree on the detailed module structure and encapsulation solutions [2].

The difficulty in obtaining useful information from short-term field tests is that performance changes are small and difficult to distinguish from measured data due to data scattering caused by variations in the measurement conditions. Factors such as irradiance level, solar spectrum and module temperature all influence measured performance parameters in different ways. This problem is normally dealt with by calculating temperature and irradiance corrections to the measured data to make all measurements comparable at the Standard Test Conditions [3,4]. Direct application of these methods to measured field data gives accurate results when sufficiently long time periods are analyzed, but the scatter of data points often makes it difficult to recognize small performance changes at an early stage of field testing. This paper presents an analysis method based on filtering of data with the aim of reducing the variance caused

by weather conditions prior to calculating temperature and irradiance corrections to performance parameters. Data filtering is always included in every analysis of field test data, the minimum filter being the selection of a certain plane-of-array irradiance range within which the analysis is to be conducted. However, the rationale behind filtering choices is hardly ever mentioned.

The method presented in this paper provides a straightforward tool for assessing the effect that different filtering choices have on the data. Comprehensive field test data for full-size CIGS modules from the EU project PYTHAGORAS (ENK5-CT-2000-00334) is used to study the effect of filtering criteria based on plane-of-array irradiance (G), module temperature (T), the ratio between global and diffuse horizontal irradiance ($R = G_H/G_D$) and the angle of incidence (θ) of sunlight on the module. It is found that methods employing thorough data filtering can give a markedly lower residual variance in measured module power (P_{mpp}), short-circuit current (I_{sc}) and open-circuit voltage (V_{oc}) than comparable data analysis methods which employ only minimal filtering. This method therefore allows smaller changes in both high- and low-irradiance performance to be detected from field measurement data and facilitates more reliable comparisons between observed changes and measured stress factors. In addition, the relationship between the error estimates of individual measurements and the data filtering results shows that the principles of operation of the measurement hardware used for gathering current-voltage data needs to be taken into account when evaluating the accuracy of P_{mpp} determination.

2. Experimental methods

2.1. Field tests

The data used in this study was measured at the Helsinki University of Technology solar energy testsite (location N 60°11', E 24°49') from the beginning of April to the end of October 2002, when the test setup consisted of sixteen 60cm•120cm CIGS modules manufactured by Würth Solar with an average aperture area efficiency of approximately 8%, tilted at an angle of 45° due south. The individual current-voltage (IV) curves of all modules and the value of G at the start of every IV-scan were recorded at ten minute intervals if the condition $G > 30 \text{ W/m}^2$ was fulfilled. Eighty points were recorded from each IV-curve with a variable electronic load, and the current and voltage corresponding to the measured point with the highest power were stored as the maximum power point current (I_{mpp}) and voltage (V_{mpp}). I_{sc} was calculated by extrapolating the measured curve to zero voltage, and V_{oc} was obtained directly from the measured data.

The error estimates pertaining to this IV-analysis for I_{sc} , V_{oc} , P_{mpp} and FF values at each irradiance level studied in this paper are shown in Table 1. The meteorological variables G , G_H , G_D and T were recorded around the clock at 10 second intervals and stored as 5 minute averages. Module temperatures were measured from one module in the middle of the measurement rack and from two modules on the opposite edges of the rack. The temperatures of the remaining modules were estimated by interpolation. The angle of incidence θ at each measurement was calculated and stored in the data files. Further details on the field test methodology can be found in [5].

Table 1: Error estimates for measured performance parameters at different plane-of-array irradiances.

| Parameter | 400 W/m ² | 600 W/m ² | 800 W/m ² | 1000 W/m ² |
|------------------|----------------------|----------------------|----------------------|-----------------------|
| I _{sc} | 0.22 % | 0.15 % | 0.11 % | 0.09 % |
| V _{oc} | 0.08 % | 0.07 % | 0.07 % | 0.07 % |
| P _{mpp} | 1.06 % | 1.14 % | 1.08 % | 1.13 % |
| FF | 1.36 % | 1.37 % | 1.26 % | 1.30 % |

2.2. Data filtering, temperature correction and analysis methods

The goal of this work was to develop a method for data filtering and temperature correction with which daily performance data can be calculated with good accuracy at any irradiance level. This requires filtering the data to find conditions which correspond to sunny conditions and a clear sky. If performance is analyzed at an irradiance G , the range of irradiance values included in the analysis have to be within a specified interval from G . A larger interval gives more measurement points but also more variation in the performance parameters. Further refinements to the filtering are obtained by restricting the values of the variables T , R and θ . Figure 1 shows every measurement point for these three variables during the test period plotted against the corresponding value of G .

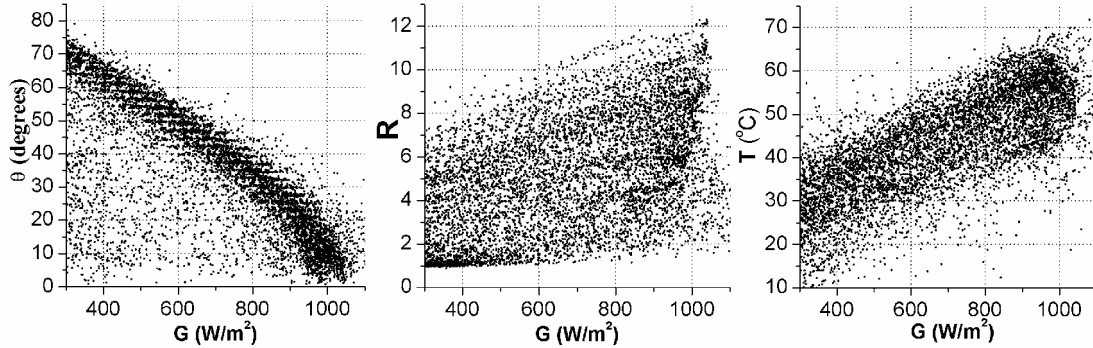


Figure 1. Distribution of filtering variables as a function of irradiance during the measurement period. Figures provide the basis for selection of suitable filtering criteria.

The plotted module temperature was taken from one module in the middle of the measurement rack. The dependence of θ on G clearly shows a high density of points along a path which defines a clear day ($\theta = \arccos[G/G_{\max}]$, where $G_{\max} \approx 1000$ W/m²), and cloudy conditions can as a first approximation be excluded by limiting the analysis to this part of the data. The variable R is used to quantify clearness with greater precision. It is seen in Figure 1 that R values are evenly spread out over the entire irradiance range with slight accumulation of high R values around $G \approx 900$ – 1000 W/m² and low values at $G \approx 300$ – 400 W/m². R is an especially important filtering parameter for I_{sc} and I_{mpp} since they are sensitive to variations in the solar spectrum. Module

temperatures fall within a range which is approximately 25°C wide and increases as a function of G. This is of significance in the calculation of temperature corrections, as the reference temperature should preferably be within the range of measured temperatures.

The analysis was performed on a database containing data from over 14,000 IV-scans for each module. The data for each scan contained the meteorological variables, T, I_{sc} , V_{oc} , I_{mpp} , V_{mpp} , FF and P_{mpp} . The irradiance-scaled parameters I_{sc}/G and I_{mpp}/G were used instead of I_{sc} and I_{mpp} in the calculations since the irradiance-dependence of current parameters is very linear. The symbol Y will be used below as a general symbol for any performance parameter. The data was of high quality with less than 0.6% of corrupt data from measurement hardware malfunctions. The goal of the data analysis was to find a method which combines data filtering and temperature correction to (A) provide as precise an estimate for the daily value of each Y at a given irradiance level G_0 as possible while (B) giving measurement data from as many days as possible. The requirements A and B are mutually restricting. The filtering was performed with all possible combinations of the filtering criteria presented in Table 2.

Table 2: Filtering parameters and criteria. In the final step, filtering was performed with all combinations of these six criteria, creating a total of 5,184 differently filtered data sets for each plane-of-array irradiance G_0 .

| Filtering parameters | Filtering criterion | Number of criteria per G_0 |
|--|---|--|
| Irradiance level (G_0) and width of irradiance interval (ΔG) | $G_0 - \Delta G/2 < G < G_0 + \Delta G/2$ with $G_0 = 400, 600, 800, 1000 \text{ W/m}^2$ and $\Delta G = 60, 80, 100 \text{ W/m}^2$ | 3 |
| Module temperature minimum (T_{min}) and maximum (T_{max}) | $T_{min} < T < T_{max}$ with $T_{min} = 10, 20, 30 \dots 60^\circ\text{C}$ and $T_{max} = T_{min} + 10^\circ\text{C}, T_{min} + 20^\circ\text{C}, T_{min} + 30^\circ\text{C}$ | 6 3 |
| Minimum of G_H/G_D ratio (R_{min}) | $R > R_{min}$ with $R_{min} = 1, 2, 3 \dots 8$ | 8 |
| Minimum (θ_{min}) and maximum (θ_{max}) angle of incidence | $\theta_{min} < \theta < \theta_{max}$ with $\theta_{min} = 0, 10, 20 \dots 50^\circ$ and $\theta_{max} = \theta_{min} + 20^\circ, \theta_{min} + 30^\circ$ | 6 2 |
| | | Π 5,184 |

The data analysis was carried out as follows: The data was filtered with variables G, R and θ and the data set (hereafter labelled Set 1) in which performance parameter Y best met requirements A and B were identified. The temperature coefficients for each Y were then calculated from Set 1 data. The data was then filtered with variables G, R, θ and T and the data sets (Set 2) in which the temperature-corrected values of each Y best met requirements A and B were identified. Finally, to evaluate the utility of the employed filtering method, the variance in Set 2 data was compared to the variance in

data obtained from a standard correction method without data filtering to see how much reduction in the scatter of data points could be achieved.

Temperature coefficients can be determined in the field by shading experiments [3] or by analyzing measurement results obtained at different temperatures. In this study, the coefficients were determined from the measured field data as follows. The formula for calculating temperature corrections to all performance parameters except FF and P_{mpp} (whose temperature corrected-values were obtained directly from the temperature-corrected values of the other parameters) was

$$Y_{REF} = \frac{Y(T)}{1 + \alpha_Y \cdot (T - T_{REF})} \quad (1)$$

where Y_{REF} is the value of Y at the reference temperature T_{REF} , $Y(T)$ is its value at temperature T, and α_Y is the temperature coefficient of Y. The analysis was carried out from 400 W/m^2 to 1000 W/m^2 at 200 W/m^2 intervals, and T_{REF} was chosen to be in the middle of the temperature distribution for each G in Figure 1; 30°C for 400 W/m^2 , 40°C for 600 W/m^2 , 45°C for 800 W/m^2 and 55°C for 1000 W/m^2 . The difficulty in calculating temperature coefficients with a least-squares fit to field measurements of a parameter Y is that a large amount of data is needed to get a reliable fit, but the value of Y may change with time which limits the time range included in the data. In this work, time was included as an independent parameter in the fitting process by defining Y_{REF} at irradiance G as a function of time:

$$Y_{REF}(G, t) = A_Y(G) + B_Y(G) \cdot t + C_Y(G) \cdot t^2, \quad (2)$$

where A_Y, B_Y and C_Y are constant for each chosen value of G and t is the time. This modification allowed the inclusion of the entire data set from April to October 2002 in the determination of the temperature coefficients. The coefficients were obtained for each irradiance level G_0 in a minimization of the following sum of squares (SS) by varying α_Y, A_Y, B_Y and C_Y :

$$SS = \sum_{i=1}^N \left(Y(G_0 \pm \Delta G, T_i, t_i) - \left(A_Y(G_0) + B_Y(G_0)t_i + C_Y(G_0)t_i^2 \right) \cdot \left(1 + \alpha_Y(G_0) \cdot (T_i - T_{REF}(G_0)) \right) \right)^2 \quad (3)$$

where $Y(G_0 \pm \Delta G, T_i, t_i)$ is the value measured at time t_i within the irradiance interval $G_0 \pm \Delta G$ at module temperature T_i and N is the total number of measurements included in the fit. Since field measurements always include some measurement errors, the fitting was performed twice and data points which differed from the fitted curve by more than 2.5 standard deviations after the first fit were eliminated from the second fit. The obtained α_Y values were then used in (1) to transform each measured Y value to Y_{REF} . Irradiance corrections were included in the calculations only in the use of the two irradiance-scaled parameters I_{sc}/G and I_{mpp}/G .

In order to select the filtering criteria which give Set 1 and Set 2 data, a computer program was written to filter the data based on the conditions in Table 2 and to perform calculations on the filtered data set. A total of 288 different combinations of filtering

criteria were used in the first step when temperature filtering was not included, and 5,184 combinations in the final step. The symbol Ω is used below to refer to a given combination of criteria from Table 2. The program performed the following calculations:

1. For each Ω , each Y , each module m and each day d , the daily standard deviation in the measured Y values, $\sigma_Y(\Omega, m, d)$, was calculated. To ensure a valid $\sigma_Y(\Omega, m, d)$ value, it was demanded that at least three IV-measurements fulfilling the criteria Ω be available from module m on day d .
2. The average of $\sigma_Y(\Omega, m, d)$ over all days, $\overline{\sigma_Y}(\Omega, m)$, was calculated for each module.
3. The average of $\overline{\sigma_Y}(\Omega, m)$ over all modules, $\overline{\sigma_Y}(\Omega)$, was calculated. To ensure that enough data had been included in the average, it was demanded that $\overline{\sigma_Y}(\Omega, m)$ be available from at least 8 modules.
4. The proportion $f(\Omega)$ of days during the measurement period which contained data contributing to $\overline{\sigma_Y}(\Omega)$ was calculated.

The utility of a given combination of filtering criteria Ω for studying changes in performance parameter Y could be evaluated when $f(\Omega)$ and $\overline{\sigma_Y}(\Omega)$ had been calculated for all Ω and were plotted against each other. The criteria A and B presented above were quantified as follows: (A) $\overline{\sigma_Y}(\Omega)$ should be as small as possible while (B) $f(\Omega)$ should be as large as possible. The first condition was based on the assumption that performance degradation during one day was negligible, and that $\overline{\sigma_Y}(\Omega)$ therefore was inversely proportional to the accuracy by which the daily value of a performance parameter could be stated in the filtered data set. The second condition expressed how well changes in Y could be followed over time. The lowest values for $\overline{\sigma_Y}(\Omega)$ always occur with strict filtering conditions which give a very small $f(\Omega)$. To obtain a higher $f(\Omega)$ filtering conditions must be relaxed, which in turn raises $\overline{\sigma_Y}(\Omega)$. The choice of the best Ω is subjective and depends on the application at hand.

3. Results

3.1. Identification of filtering criteria for Set 1 data

Selection of Set 1 data was done for two performance parameters, V_{oc} and I_{sc}/G . Temperature coefficients for V_{mpp} and I_{mpp}/G were calculated from the same set of data as those of V_{oc} and I_{sc}/G , respectively. Figure 2 shows $\overline{\sigma_Y}(\Omega)$ versus $f(\Omega)$ for four values of G_0 . Some data points with high $\overline{\sigma_Y}(\Omega)$ have been excluded from the Figure

for clarity. It can be seen that $\overline{\sigma_Y}(\Omega)$ is smaller for V_{oc} than for I_{sc}/G at every irradiance except 1000 W/m^2 . The magnitude of $\overline{\sigma_Y}(\Omega)$ decreases as a function of irradiance for both V_{oc} and I_{sc}/G . The points representing the Ω which were chosen for calculation of temperature coefficients have been encircled in Figure 2 and the filtering criteria of these Ω are shown in Table 3. The condition $f(\Omega) > 30\%$ was used as the selection criterion together with a small $\overline{\sigma_Y}(\Omega)$ value.

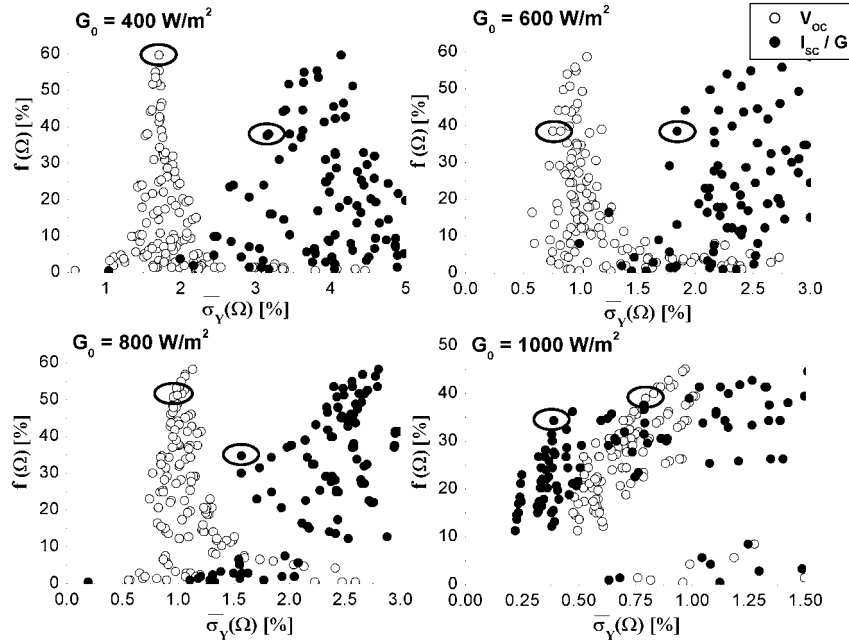


Figure 2. Average daily standard deviation in V_{oc} and I_{sc}/G versus frequency of observation for different combinations (Ω) of filtering criteria on G , R and θ . Each point represents one Ω . The points representing the best criteria have been encircled.

3.2. Temperature coefficients

Filtering was performed on the data according to the conditions in Table 3, and temperature coefficients were calculated at each irradiance level from the filtered data set for V_{oc} , V_{mpp} , I_{sc}/G and I_{mpp}/G . Differences in coefficients between modules were significant. Table 4 shows, for each performance parameter, the average of the coefficients and the standard deviation in the coefficients over all modules. It is worth noting that the irradiance sensitivity of I_{sc}/G and I_{mpp}/G adds significant uncertainty to their temperature coefficients at 400 W/m^2 since the analyzed data was primarily gathered early in the morning and late in the afternoon. Filtering based on R may not limit the spectral variation sufficiently, and a small misalignment of the plane-of-array irradiance sensor would create a systematic difference between I_{sc}/G and I_{mpp}/G values measured in the morning and the afternoon. This would influence the temperature coefficients since afternoon module temperatures at 400 W/m^2 were in these field tests on the average about 5°C higher than morning temperatures. At 600 W/m^2 and above, the calculated I_{sc}/G and I_{mpp}/G temperature coefficients are reliable since the spectrum

varies less and there is no significant temperature difference between morning and afternoon data.

Table 3: Filtering criteria employed in the calculation of temperature coefficients for I_{sc} , I_{mpp} , V_{oc} and V_{mpp} . The criteria correspond to the circled points in Figure 2.

| G_0 (W/m^2) | Y | ΔG (W/m^2) | R_{min} (-) | θ_{min} ($^\circ$) | θ_{max} ($^\circ$) |
|----------------------|--------------|---------------------------|------------------|--------------------------------|--------------------------------|
| 400 | I_{sc} / G | 100 | 4 | 50 | 70 |
| | V_{oc} | 100 | 1 | 40 | 70 |
| 600 | I_{sc} / G | 100 | 5 | 40 | 70 |
| | V_{oc} | 100 | 5 | 40 | 70 |
| 800 | I_{sc} / G | 100 | 5 | 30 | 60 |
| | V_{oc} | 100 | 3 | 20 | 40 |
| 1000 | I_{sc} / G | 100 | 5 | 0 | 20 |
| | V_{oc} | 100 | 4 | 0 | 20 |

Table 4: Temperature coefficient averages and standard deviation between modules at four irradiance levels, calculated from Set 1 data. I_{sc}/G and I_{mpp}/G temperature coefficients at $400 W/m^2$ are subject to high uncertainty.

| G_0 (W/m^2) | Y | α_Y AVERAGE (% / $^\circ C$) | α_Y STDEV (% / $^\circ C$) |
|----------------------|---------------|---|---------------------------------------|
| 400 | I_{sc} / G | -0.167 | 0.123 |
| | I_{mpp} / G | -0.155 | 0.167 |
| | V_{oc} | -0.321 | 0.042 |
| | V_{mpp} | -0.317 | 0.128 |
| 600 | I_{sc} / G | 0.036 | 0.048 |
| | I_{mpp} / G | 0.068 | 0.072 |
| | V_{oc} | -0.321 | 0.038 |
| | V_{mpp} | -0.363 | 0.077 |
| 800 | I_{sc} / G | 0.058 | 0.032 |
| | I_{mpp} / G | 0.066 | 0.061 |
| | V_{oc} | -0.328 | 0.028 |
| | V_{mpp} | -0.400 | 0.054 |
| 1000 | I_{sc} / G | 0.066 | 0.028 |
| | I_{mpp} / G | 0.066 | 0.064 |
| | V_{oc} | -0.325 | 0.030 |
| | V_{mpp} | -0.407 | 0.051 |

3.3. Identification of filtering criteria for Set 2 data

Figure 3 shows $\overline{\sigma_Y}(\Omega)$ versus $f(\Omega)$ plots for the temperature-corrected values of V_{oc} , FF, I_{sc}/G and P_{mpp}/G at $G_0 = 400 \text{ W/m}^2$ and 600 W/m^2 . At 400 W/m^2 , the $f(\Omega)$ values begin to rise rapidly for V_{oc} and FF as $\overline{\sigma_Y}(\Omega)$ reaches values of 1.25% and 2%, respectively. For I_{sc}/G and P_{mpp}/G , $f(\Omega)$ increases at $\overline{\sigma_Y}(\Omega) > 3\%$ and 6% , which indicates that assessing the values of I_{sc} and P_{mpp} can not be done with good precision at very low irradiance. At 600 W/m^2 the precision is markedly improved for all variables, V_{oc} and FF yield large $f(\Omega)$ values at deviations between 0.5% – 1% while I_{sc}/G and P_{mpp}/G show deviations of 1% and 2.5% when $f(\Omega)$ begins to rise.

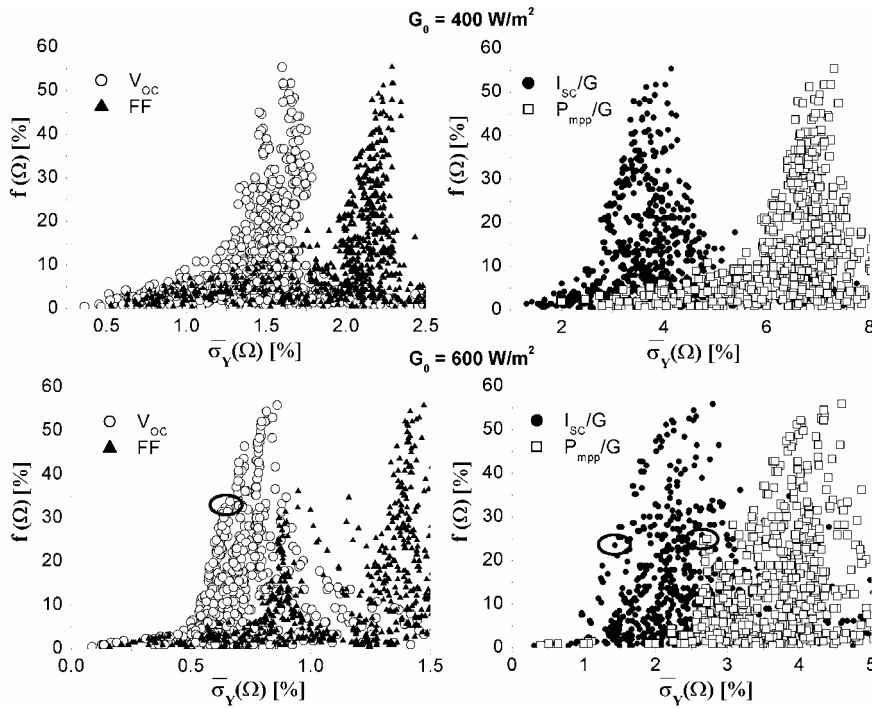


Figure 3. Average daily standard deviation of temperature-corrected performance parameters versus frequency of observation for different combinations (Ω) of filtering criteria on G , T , R and θ at $G_0 = 400 \text{ W/m}^2$ and 600 W/m^2 . Each point represents one Ω . The points used in the method comparison for $G_0 = 600 \text{ W/m}^2$ have been encircled.

Figure 4 shows the same plots at $G_0 = 800 \text{ W/m}^2$ and 1000 W/m^2 . Large $f(\Omega)$ values at 800 W/m^2 are obtained when $\overline{\sigma_Y}(\Omega) > 0.25\% - 0.3\%$ for V_{oc} and FF, and when $\overline{\sigma_Y}(\Omega) > 0.5\%$ and $\overline{\sigma_Y}(\Omega) > 1\%$ for I_{sc}/G and P_{mpp}/G , respectively. At 1000 W/m^2 the rise in $f(\Omega)$ occurs at $\overline{\sigma_Y}(\Omega) \approx 0.1\%$ for V_{oc} and FF and $\overline{\sigma_Y}(\Omega) \approx 0.2\%$ for I_{sc}/G and P_{mpp}/G . In general, an increase of 200 W/m^2 in the irradiance level gives a relative improvement in $\overline{\sigma_Y}(\Omega)$ of approximately 50%. For reasons to be explained later, a comparison

between the data in Figures 3 and 4 to that in Table 1 shows that many $\overline{\sigma_{FF}}$ values are lower than the estimated FF measurement error, and $\overline{\sigma_{P_{mpp}}}$ values are lower than the P_{mpp} error at 800 and 1000 W/m².

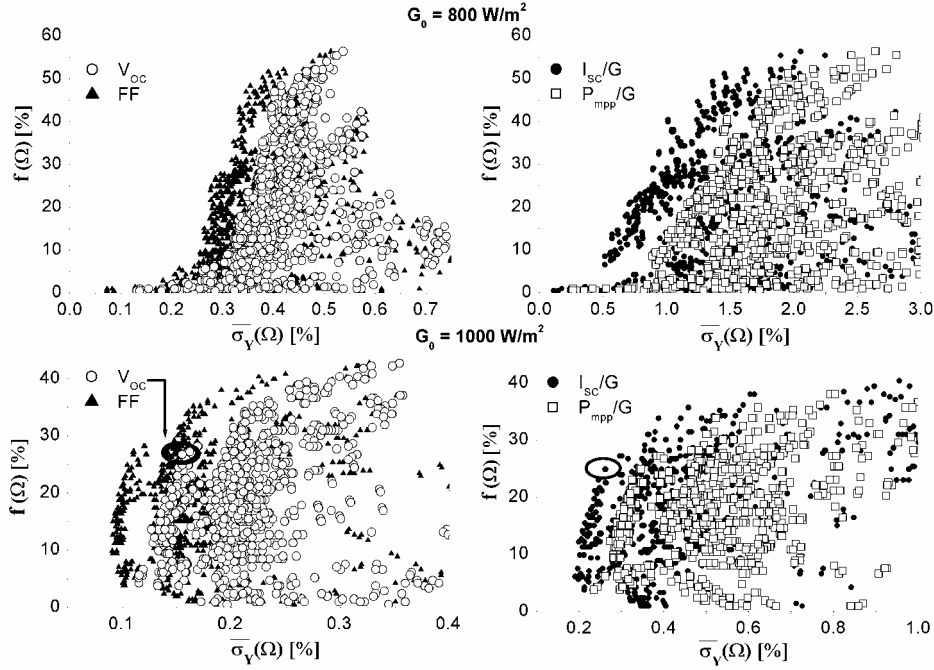


Figure 4. Average daily standard deviation of temperature-corrected performance parameters versus frequency of observation for different combinations (Ω) of filtering criteria on G , T , R and θ at $G_0 = 800 \text{ W/m}^2$ and 1000 W/m^2 . Each point represents one Ω . The points used in the method comparison for $G_0 = 1000 \text{ W/m}^2$ have been encircled.

3.4. Comparison between different methods for performance evaluation

In order to compare performance parameter predictions made with the method presented in this paper (referred to as method A) to that which is obtained with a standard method which includes only minimal data filtering (method B), the time series of the performance parameters measured from one randomly selected module were calculated at irradiances of 600 W/m² and 1000 W/m² with both methods. The filtering conditions at 600 W/m² and 1000 W/m² corresponding to the circled points in Figures 3 and 4 were chosen as the best ones based on the selection criteria $f(\Omega) > 20\%$ and a small $\overline{\sigma_V}(\Omega)$. The conditions corresponding to the circled points are presented in Table 5. The selection was made only for parameters with $\overline{\sigma_V}$ values larger than their measurement error estimates.

Table 5: The best filtering criteria at $G_0 = 600 \text{ W/m}^2$ and 1000 W/m^2 , which correspond to the circled points in Figures 3 and 4.

| G_0 (W/m^2) | Y | ΔG (W/m^2) | T_{\min} | T_{\max} | R_{\min} (-) | θ_{\min} ($^\circ$) | θ_{\max} ($^\circ$) |
|-----------------------------|--------------|----------------------------------|------------|------------|-------------------|---------------------------------|---------------------------------|
| 600 | V_{oc} | 80 | 30 | 50 | 3 | 40 | 60 |
| | I_{sc} / G | 100 | 30 | 60 | 3 | 30 | 50 |
| | P_{mpp} | 100 | 30 | 60 | 3 | 30 | 50 |
| 1000 | V_{oc} | 100 | 30 | 60 | 4 | 0 | 10 |
| | I_{sc} / G | 100 | 30 | 60 | 5 | 0 | 10 |

In method A, data filtering was performed according to these conditions and temperature corrections were calculated with the module-specific temperature coefficients from section 3.2. In method B, the only filtering was performed in the selection of the analyzed data within an irradiance interval of $\pm 50 \text{ W/m}^2$ from the irradiance level under study. The temperature coefficients of the studied module were calculated in method B for I_{sc}/G , I_{mpp}/G , V_{oc} and V_{mpp} at 1000 W/m^2 by performing a linear fit corresponding to equation 1 to the entire data set and using 25°C as the reference temperature. These coefficients were assumed to be independent of irradiance and were used at both 600 W/m^2 and 1000 W/m^2 . In both methods, a daily average of each temperature-corrected performance parameter was calculated for all days with at least 3 measurements.

The resulting data points for $G_0 = 600 \text{ W/m}^2$ are plotted in Figure 5 and for $G_0 = 1000 \text{ W/m}^2$ in Figure 6. I_{sc}/G and P_{mpp}/G values have been multiplied with G_0 to give correct units. For convenience, these products are referred to simply as I_{sc} and P_{mpp} below. In both Figures, it is seen that method A gives less scattering of data points than method B for P_{mpp} , V_{oc} and I_{sc} . In some cases, the data given by methods A and B trace different arcs because the data which was excluded in the filtering process in method A influences the data in method B. The differences between the two methods was quantified by comparing the residual variance $V_Y = \text{Var}(Y) \cdot (1 - r^2)$, where $\text{Var}(Y)$ is the Variance in Y when time-dependence is not taken into account and r^2 is the coefficient of determination of a linear fit to the data points between May and October. The results are shown in Table 6 as the ratio V_Y^A/V_Y^B together with the ratio f_A/f_B , which shows how much the number of days with measurement data points is reduced in the filtering process. It is seen that method A is superior over method B in all comparisons, but especially in evaluating V_{oc} at 600 W/m^2 and I_{sc} at 1000 W/m^2 . The reduction in residual variance is in general larger than the loss in measurement days.

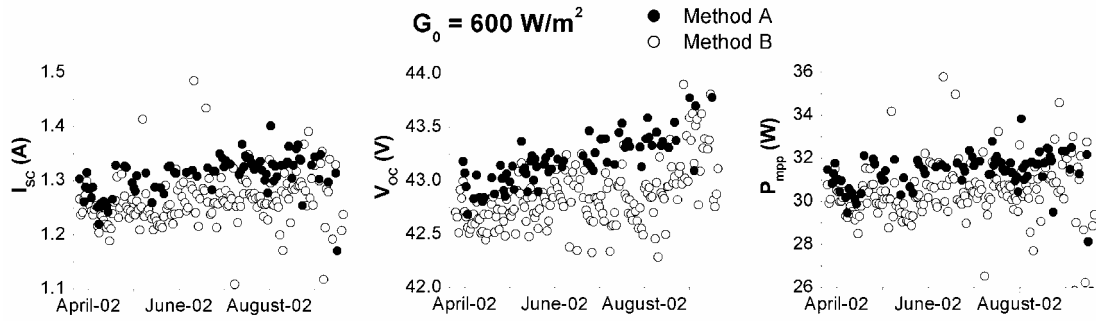


Figure 5. Evaluation of performance parameters with method A and method B at 600 W/m^2 . Method A shows less scattering of data points all performance parameters.

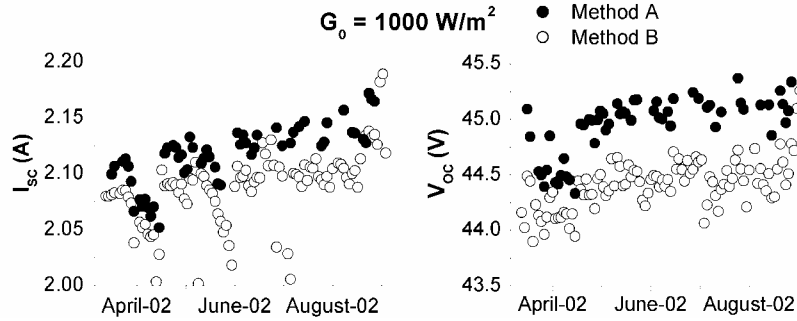


Figure 6. Evaluation of performance parameters with method A and method B at 1000 W/m^2 . Method A shows less scattering of data points for both I_{sc} and V_{oc} . The reduction in the number of days with measurement data is also evident.

Table 6: Comparison between the accuracy of methods A and B. The table shows the ratio between the residual variances V_Y^A and V_Y^B of a linear fit to each group of data points and the corresponding ratio f_A/f_B between the number of days with measurement data for both methods.

| G_0 (W/m^2) | Y | V_Y^A/V_Y^B | f_A/f_B |
|-----------------------------|-----------|---------------|-----------|
| 600 | V_{oc} | 0.272 | 0.418 |
| | I_{sc} | 0.394 | 0.459 |
| | P_{mpp} | 0.322 | 0.459 |
| 1000 | V_{oc} | 0.604 | 0.539 |
| | I_{sc} | 0.213 | 0.539 |

4. Some observations on the method

In the previous section it was shown that the method based on data filtering presented in this paper gives clearly less scattering in performance parameter data than the simpler method which was chosen for reference. The other consequence of filtering the data is that the number of data points is reduced, which is also evident in Figures 5 and 6. The relationship between data scattering and number of points is the one illustrated in Figures 3 and 4, and these plots can thus be used to find a data set with a suitable combination for any analysis of performance changes in field tests. The $f(\Omega)$ vs $\overline{\sigma_Y}(\Omega)$ can be improved by calculating them separately for each studied module. It is also worth noting that the time distribution of measurement points after filtering may be uneven particularly when narrow filters for θ are chosen. The values of θ which occur during different seasons should be compared with filtering conditions to ensure that no season is eliminated entirely from the resulting data set.

The function $f(\Omega)$ depends only on the site at which the modules are deployed, whereas $\overline{\sigma_Y}(\Omega)$ is to a large degree a module-specific function. If the effect of the different filtering parameters contained in Ω on $\overline{\sigma_Y}(\Omega)$ is known, good filtering conditions can be chosen directly from meteorological measurements which give $f(\Omega)$. An analytical function which represents $\overline{\sigma_Y}(G_0, \Delta G, T_{\min}, T_{\max}, R_{\min}, \theta_{\min}, \theta_{\max})$ with sufficient accuracy was not obtainable from the data used in this work, but the following guidelines can be given for filtering of data from the studied CIGS modules. Using a narrow temperature interval rarely gives a significantly lower $\overline{\sigma_Y}(\Omega)$ for any Y . This implies that all temperature-corrected parameters obey a linear temperature dependence, and the widest interval (in this study; $T_{\max} - T_{\min} = 30^\circ\text{C}$) is usually preferable since it gives the highest $f(\Omega)$. For filtering conditions on θ , the best results are found in the interval corresponding to a clear day, visible in Figure 1. Filtering based on ΔG and R_{\min} gives more variation, and the effects of these two criteria on the $\overline{\sigma_Y}$ values at different irradiance levels are summarized in Table 7. These guidelines give an indication of which performance parameters are affected by the choice of certain filtering conditions for the CIGS modules tested in this work. Application of this method to other module technologies and test sites requires the calculation and comparison of the corresponding $\overline{\sigma_Y}(\Omega)$ and $f(\Omega)$ functions.

Finally, it was noted in section 3.3. that the average daily standard deviation of FF and P_{mpp} calculated in Figures 3 and 4 was in some cases significantly less than the estimated measurement error. This is explained by the operation of the electronic load used in scanning the IV-curves. For given values of I_{sc} and V_{oc} , the current-voltage pairs on the IV-curve which are recorded in the measurement will be very nearly identical in different IV-scans, which gives a low standard deviation and therefore an apparent accuracy higher than the real accuracy of the maximum power point determination. Within the limits set by the measurement equipment, the real accuracy can be increased by increasing the number of measurement points. In the measurement setup used in this

study, a quadrupling of the number of measurement points to 320 would have yielded error estimates from the IV-analysis slightly below 0.5% for FF and 0.3% for P_{mpp} .

Table 7: Summary of the effect of filtering criteria ΔG and R_{min} on f and on the $\overline{\sigma_Y}$ values of the CIGS modules measured in this field test.

| G_0 (W/m^2) | Filtering criterion | f | $\overline{\sigma_{Voc}}$ | $\overline{\sigma_{Isc}}$ | $\overline{\sigma_{FF}}$ | $\overline{\sigma_{Pmpp}}$ |
|-------------------|------------------------------------|--------------------------------------|---|--|---|--|
| 400 | ΔG (60/80/100 W/m^2) | $\Delta G=60$ severely restricts f | $\Delta G=60$ gives slightly lower values | No effect | No effect | No effect |
| | R_{min} (1-8) | $R_{min} > 4$ severely restricts f | $R_{min} \leq 2$ gives lower values | Higher R_{min} gives lower values | $R_{min} \leq 2$ gives lower values | $R_{min} \leq 2$ gives lower values |
| 600 | ΔG | $\Delta G=60$ restricts f | $\Delta G=60$ gives slightly lower values | $\Delta G=60$ gives higher values | No effect | $\Delta G=60$ gives slightly higher values |
| | R_{min} | $R_{min} > 5$ severely restricts f | No effect | Higher R_{min} gives lower values | Higher R_{min} gives higher values | No effect |
| 800 | ΔG | No Effect | No effect | $\Delta G=60$ gives slightly higher values | No effect | $\Delta G=60$ gives slightly higher values |
| | R_{min} | $R_{min} > 6$ restricts f | No effect | Higher R_{min} gives lower values | No effect | Higher R_{min} gives slightly lower values |
| 1000 | ΔG | No effect | No effect | No effect | $\Delta G=60$ gives slightly lower values | No effect |
| | R_{min} | $R_{min} > 6$ restricts f | No effect | Higher R_{min} gives slightly lower values | No effect | Higher R_{min} gives slightly lower values |

5. Summary and conclusions

In this work, a data filtering methodology for improving the evaluation of performance parameters in field tested PV modules was developed and applied to CIGS technology. The methodology is a valuable tool in field testing since every analysis of PV field data must employ data filtering to some degree and because it is equally applicable to any PV technology. Different filtering conditions were compared to each other based on how accurately a given performance parameter can be evaluated in the filtered data set [$\overline{\sigma_Y}(\Omega)$] and how many days of data are available after filtering [$f(\Omega)$]. The best filters are a matter of subjective choice depending on the application. The choice of filters for the example presented in this paper yielded, at an irradiance of 1000 W/m^2 , a 40% lower residual variance in V_{oc} and a 79% lower residual variance in I_{sc} than what was obtained with a regular temperature and irradiance correction method. The number of days with measurement data was reduced by 46% by the same filtering conditions. Medium irradiance (600 W/m^2) results showed reductions in the residual variance of P_{mpp} (68%), I_{sc} (61%) and V_{oc} (73%) significantly larger than the loss of measurement days (54-58%). This shows that significant reductions of data scattering can be obtained

when the analysis is confined to specified intervals of basic meteorological and module parameters.

Results presented in this paper also show that the apparent accuracy (as represented by the standard deviation) of fill factor and P_{mpp} measurements may be misleading if the number of IV-points gathered in the measurement is insufficient. This should be taken into account in the planning of field test measurements. In conjunction with the performance evaluation presented in this paper, a method for calculating temperature coefficients directly from field measurement data was presented. Using time as an independent variable when a least squares fit is performed reduces the time-dependent variation which would affect the fit strongly if data from a long time period is used. Reliable temperature coefficients for voltage parameters can be obtained at plane-of-array irradiances as low as 400 W/m^2 , whereas for current parameters 600 W/m^2 was the practical lower limit in this study.

With the help of the methodology presented in this paper, changes in the performance of field tested modules can be detected with greater accuracy than with methods which employ only minimal filtering of data. This not only makes it possible to detect changes at an earlier stage of testing, but also facilitates better comparisons between observed changes in performance parameters and measured stress factors such as high module temperature peaks, temperature cycles or unusually high insolation. If correlations between stress factors and performance changes are found, the necessary feedback for accelerated ageing tests in the laboratory can be given directly and future module designs improved.

Acknowledgements

Svenska Litteratursällskapet i Finland rf is gratefully acknowledged for financial support.

References

1. Czanderna A, Jorgensen G. Accelerated life testing and service lifetime prediction for PV technologies in the twenty-first century. *Electrochemical Society Proceedings 99-11 (Photovoltaics for the 21st century)* 1999; 57-67.
2. McMahon T. Accelerated testing and failure of thin-film PV modules. *Progress in Photovoltaics: Research and Applications* 2004; **12** (2-3): 235-248. DOI: 10.1002/pip.526
3. King D, Kratochvil J, Boyson W. Temperature coefficients for PV modules and arrays: measurement methods, difficulties and results. *Proceedings of the 26th IEEE PVSC* 1997; 1183-1186.
4. Kurtz S, Myers D, Townsend T, Whitaker C, Maish A, Hulstrom A, Emery K. Outdoor rating conditions for photovoltaic modules and systems. *Solar Energy Materials and Solar Cells* 2000; **62** (4): 379-391.

5. Moring H-D, Stellbogen D, Schäffler R, Oelting S, Gegenwart R, Kontinen P, Carlsson T, Cendagorta M, Herrmann W. Outdoor performance of polycrystalline thin film PV modules in different European climates. *Proceedings of the 19th European Photovoltaic Solar Energy Conference*, 2004; 2098-2101.